Design optimization of plate heat exchanger absorbers and desorbers for hybrid absorption compression heat pumps

Mancini, Roberta; Jensen, Jonas Kjær; Reinholdt, Lars; Markussen, Wiebke Brix; Elmegaard, Brian

Published in:
Proceedings of ECOS 2019: 32nd International Conference on Efficiency, Cost, Optimization, Simulation and Environmental Impact of Energy Systems

Publication date:
2019

Document Version
Publisher's PDF, also known as Version of record

Design optimization of plate heat exchanger absorbers and desorbers for hybrid absorption compression heat pumps

***Roberta Mancini*[a], *Jonas Kjær Jensen*[b], *Lars Reinholdt*[c], *Wiebke Brix Markussen*[d], *Brian Elmegaard*[e]**

[a] *Technical University of Denmark, Kgs. Lyngby, Denmark, robman@mek.dtu.dk*
[b] *Technical University of Denmark, Kgs. Lyngby, Denmark, jkjje@mek.dtu.dk*
[c] *Danish Technological Institute, Aarhus, Denmark, lre@teknologisk.dk*
[d] *Technical University of Denmark, Kgs. Lyngby, Denmark, wb@mek.dtu.dk*
[e] *Technical University of Denmark, Kgs. Lyngby, Denmark, be@mek.dtu.dk*

Abstract:
Design optimization of absorber and desorber in hybrid absorption compression heat pumps (HACHPs) is of paramount importance to reduce the installation costs of these systems. This paper presents a simulation framework to optimize the design of plate heat exchangers (PHEs) to be used as absorption and desorption units in HACHPs. A case study of a single-stage HACHP was chosen as an example to utilize the framework. A PHE design model was coupled with a cycle design tool, and the trade-off between heat transfer area and pressure drop in both absorber and desorber was established by estimating the impact of pressure drops on the heat pump thermodynamic performance. Corrugation geometry, plate size and count were selected as design variables for the optimization procedure, in order to obtain a diversified range of optimal solutions. It was found that the desorber pressure drop entails a higher degradation of the thermodynamic performance compared to the absorber, and the two limits of maximum allowable pressure drops of 15 kPa and 35 kPa were selected. The design optimization showed that it is preferred to choose corrugation geometry parameters, such as chevron angle, corrugation pitch and height, with the aim of enhancing the heat transfer at the expense of pressure drop. On the other hand, a diverse range of plate size and count was obtained as output of optimization. The results demonstrate how to select optimal configurations of PHE absorber and desorber for HACHPs.

Keywords:
Heat pumps, Ammonia/water, Heat transfer area, Pressure drop, Single-unit plate heat exchangers

1. Introduction

Hybrid Absorption Compression Heat Pumps (HACHPs) are a promising solution to increase the temperature of heat supply of industrial heat pumps. The use of HACHPs with ammonia/water aims at enhancing the heat pump Coefficient of Performance (COP) by replacing isothermal evaporation and condensation with the non-isothermal desorption and absorption processes of zeotropic mixtures, typically ammonia/water. By matching the temperature glide during desorption/absorption with the temperature profiles of the heat source/sink, it is possible to approach the Lorenz cycle [1], which results in an increased COP due to lower entropy generation due to finite temperature difference heat transfer in the heat exchangers (HEXs). An additional advantage is the lower saturation pressure of ammonia/water compared to pure ammonia, thus enabling a higher heat supply temperature at a lower operating pressure.
Nordtvedt [2] tested a prototype of HACHP with ammonia/water, reaching an experimental heating COP of 2.47 for supplying heat at 93 °C with an inlet source temperature of 50 °C. The experimental campaign allowed understanding of the key parameters for cycle design, i.e. the solution circulation ratio, intermediate pressure for two-stage cycles and system charge. Kim et al. [3] experimentally tested a 10 kW HACHP delivering heat at 90 °C, showing that the ammonia concentration of the lean solution can be optimized according to the working conditions, e.g. heat supply temperature and capacity. Jensen et al. [4, 5] further investigated the feasibility and working domains of HACHPs by means of numerical modelling. The circulation ratio, defined as the ratio f between the mass flow rates of the lean solution and the rich solution, was found as a design parameter to optimize for each rich ammonia mass fraction x_r. The maximum heat supply temperature for single-stage cycles was found to be 111 °C with standard refrigeration components, and 147 °C with transcritical CO_2 components. Liu [6] further assessed the feasibility of HACHPs for delivering saturated steam at 0.5 MPa. Wersland et al. [7] compared single-stage HACHPs utilizing screw compressors against a two-stage cycle with piston compressors, showing that the two-stage cycle with intercooling outperformed the single-stage configuration with a COP increase of 22.5 %. In addition to literature studies, HACHPs started to be implemented as a commercial solution for a number of applications, i.e. waste heat recovery and high temperature heat supply for industrial processes [8].
In HACHPs, absorber and desorber design is of paramount importance to attain temperature glide matching between the ammonia/water mixture and the heat source/sink. Compact HEX configurations are preferred compared to shell and tube HEXs, in order to reduce the investment due to large heat transfer area. In this context, plate heat exchangers (PHEs) constitute an advantageous configuration for both absorber and desorber units to reduce the size of the system at high thermal effectiveness. PHEs are comprised of thin corrugated parallel plates, stacked together to form parallel channels for co- or counter-current flow arrangement. PHEs were installed in the experimental set-ups of both Nordtvedt [2] and Kim et al. [3]. In both cases, two PHE absorbers connected in series were installed. The same was done for the desorber unit in the case of Nordtvedt [2]. According to Nordtvedt, the need to install two absorbers in series arose from difficulties in testing one single unit at the established design conditions, and possible issues were identified as liquid/vapour distribution at the inlet of the channels, as well as incomplete surface wetting of the liquid solution. In the previous experimental work, a

standard plate size from commercial manufactures was however considered in the design process for both components, and no sensitivity study or geometry optimization was carried out. The utilization of two units in series impacts the economic feasibility of HACHPs negatively, due to higher installation costs for the HEXs.

In a numerical study by Jensen et al. [9], the influence of different PHE design variables on the heat transfer and pressure drop performance was studied. Different correlations were tested for estimation of transport properties, as well as heat transfer coefficient and friction factor. This study started to put the focus on the need for a systematic full geometry optimization to design PHE absorbers and desorbers with good heat transfer characteristics and limited pressure drop.

In this context, the objective of this work is to present a simulation framework that is able to propose optimized configurations of PHE absorbers and desorbers. The utilization of the framework is demonstrated by applying it to a case study of a single-stage HACHP. In the case study, a HACHP was first sized to supply heat at 100 °C, starting from a heat source inlet temperature of 75 °C. The ammonia mass fraction of the rich solution x_r and the circulation ratio f were fixed. The full cycle specifications were thus estimated and used in order to carry out the design of PHEs as both absorber and desorber units. The design was performed by optimizing all the geometrical specification of PHEs with respect to heat transfer area and pressure drop, and by evaluating the impact of the absorber and desorber pressure drops on the cycle COP. This study should thus be seen as an attempt to develop a procedure to obtain optimized configurations of absorber and desorber, which could subsequently be tested as single units, thus targeting the reduction of installation costs of the HEXs.

2. Methods

This section describes the chosen case study, the numerical modelling for PHE design and cycle analysis, as well as the optimization problem settings. The flowchart of the overall procedure is reported in Fig. 1. All the models were developed in the MATLAB 2017b [10] simulation environment. First, the case study boundary conditions (BCs) were defined in terms of desired temperature of heat supply, heat pump capacity and temperature lift.

A cycle model, previously presented in [4], carried out the cycle design, thus estimating the pressure levels, the ammonia/water mass flow rates, as well as the inlet and outlet thermodynamics of ammonia/water and heat source/sink, needed for the PHE design. These values were sent to the optimization routines for absorbers and desorbers.

The optimization was carried out by using the MATLAB built-in genetic algorithm *gamultiobj (ga)* [10], and setting the minimization of heat transfer area and ammonia/water pressure drop as objective functions. The optimization procedure carried out the sizing of absorber/desorber for different combinations of design variables, by means of a PHE sizing model, previously published in [11]. Upper and lower bounds for all the design variables were defined in order to ensure feasible combinations of PHE design parameters, and different PHE designs were obtained at different trade-offs. In order to define different optimized PHE designs for both absorber and desorber units, the impact of ammonia/water pressure drop on COP for each configuration was estimated.

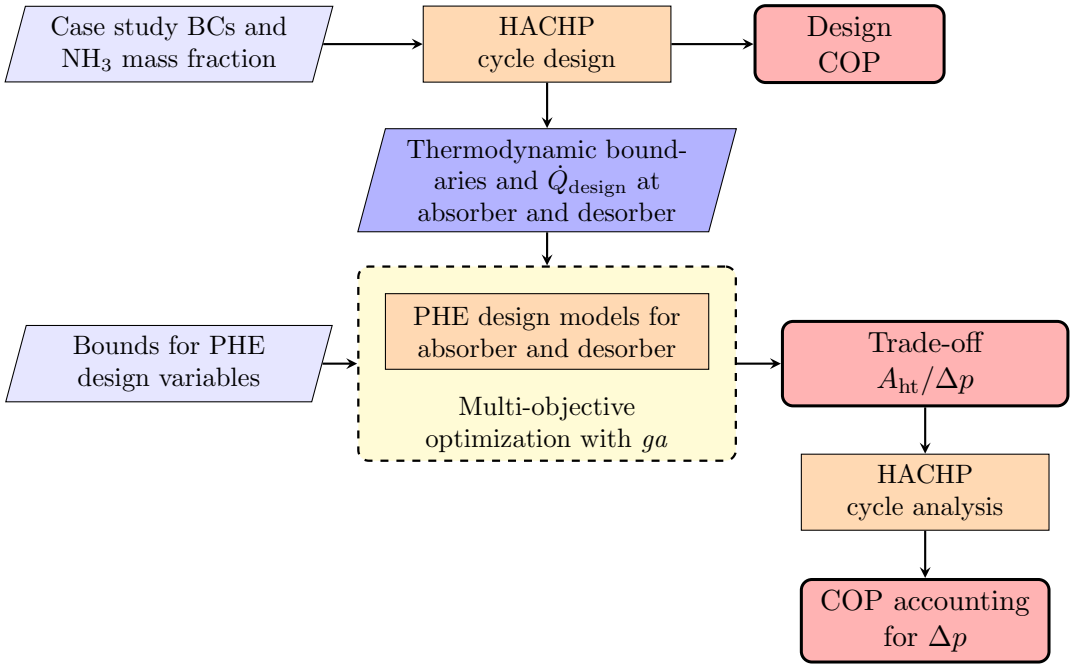

Figure 1: Work flow of the overall procedure

2.1. Case study and cycle modelling

The case study was given by a single-stage HACHP to deliver heat at 100 °C. Fig. 2 shows the schematic of the cycle, with an internal HEX to preheat the lean ammonia/water solution after the pump and a gas cooler (GC) to decrease the temperature of the ammonia vapour before the mixer. The inputs for cycle design are reported in Table 1. The circulation ratio f was found as the value maximizing the heat pump COP for the given ammonia mass fraction x_r. The sizing was carried out by fixing the heat load of the sink to the design heat flow rate of 84.0 kW. The temperature lift ΔT_{lift}, defined as the difference between the heat supply temperature ($T_{\text{sink,out}}$) and the source inlet temperature, was fixed to 25 K. The temperature levels of inlet and outlet of both sink and source are reported in the first columns of Table 1. Water was the considered medium for both heat sink and source.

The components were modelled by assuming isentropic, volumetric and electric efficiencies for compressor and pump, thermal effectiveness for IHEX and GC, and minimum temperature differences between ammonia/water and sink/source in both absorber and desorber. The thermodynamic performance of the cycle was estimated by calculating the COP as:

$$\text{COP} = \frac{\dot{Q}_{\text{abs}} + \dot{Q}_{\text{GC}}}{\dfrac{\dot{W}_{\text{comp}}}{\eta_{\text{el,comp}}} + \dfrac{\dot{W}_{\text{pump}}}{\eta_{\text{el,pump}}}} \tag{1}$$

where the sum of the heat flow rates at absorber and gas cooler is equal to the total heat flow rate at the sink $\dot{Q}_{\text{sink}}$. The same cycle model was also utilized for the estimation of cycle performance with pressure drop in absorber and desorber, i.e. the HACHP cycle analysis

showed in Fig. 1. The reader is referred to [4] for a detailed description of the HACHP cycle model.

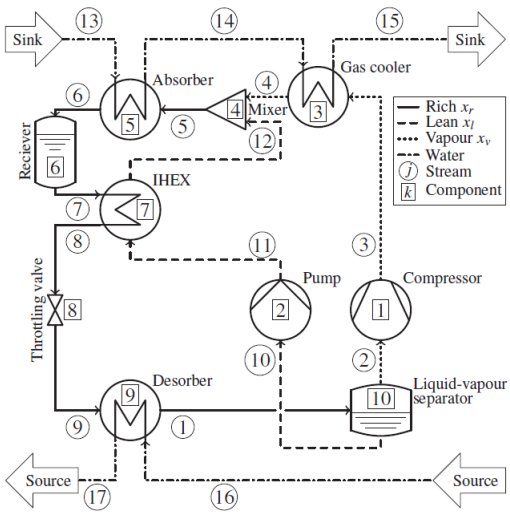

Figure 2: Schematic of the cycle [4]

Table 1: Input parameters for HACHP cycle design

Cycle			Components		
x_r	-	0.90	$\eta_{\text{is,comp}}$	-	0.75
f	-	0.39	$\eta_{\text{vol,comp}}$	-	0.90
$\dot{m}_{\text{sink}}$	kg/s	1	$\eta_{\text{el,comp}}$	-	0.90
$\dot{Q}_{\text{sink}}$	kW	84	$\eta_{\text{is,pump}}$	-	0.75
$T_{\text{sink,in}}$	°C	80	$\eta_{\text{el,pump}}$	-	0.90
$T_{\text{sink,out}}$	°C	100	ϵ_{IHEX}	-	0.85
$T_{\text{hs,in}}$	°C	75	ϵ_{GC}	-	0.85
$T_{\text{hs,out}}$	°C	65	$\Delta T_{\text{pp,abs}}$	K	5
ΔT_{lift}	K	25	$\Delta T_{\text{pp,des}}$	K	5

2.2. PHE design model

The PHE design models for both absorber and desorber were based on a one-dimensional discretization of the HEX along the flow direction at constant enthalpy steps. The solver was based on a successive substitution approach, with heat transfer area and pressure drop set as iteration variables. A total number of $n = 50$ control volumes was chosen, with tolerance set on the L2-norm of the relative residuals of plate length and pressure drop equal to 10^{-4}. The models received as input all the geometrical parameters of the PHE but the plate length, which was calculated to meet the design heat transfer rate. The reader is referred to [11] for a more detailed explanation of the models. Fluid thermo-physical properties were estimated by REFPROP 10 [12]. The following assumptions were used: (i)steady-state operating conditions, (ii) adiabatic end plates, (iii) no longitudinal conduction through the walls, (iv) no pressure drop in the manifold and (v) homogeneous model for the liquid and vapour phases.
The local heat transfer coefficient and frictional pressure drop were computed by experimental correlations. Heat transfer coefficient and pressure drop for single-phase flow of the sink/source were estimated by Martin [13]. The two-phase heat transfer coefficient of ammonia/water was estimated by Taboas et al. [14] for desorption, while the Silver [15] and Bell-Ghaly [16] method was applied for absorption. In the latter, the correlation of Zhang et al. [17] was applied to estimate the ideal pure fluid heat transfer coefficient. The frictional pressure drop during desorption was estimated by applying the Lockhart-Martinelli [18] method with single-phase friction factor and Chisholm's coefficient as suggested in [14]. The two-phase frictional pressure drop during absorption was instead estimated by Zhang et al. [17].
Transport properties of ammonia/water, namely viscosity and thermal conductivity of both liquid and vapour phases, were estimated by prediction methods from the literature. Conde-

Petit [19] was applied to estimate liquid viscosity and conductivity, as well as mixture surface tension. Wilke [20] and Mason and Saxena [21] were used to compute the vapour viscosity and thermal conductivity, respectively.

2.3. Design optimization

The design models for both absorber and desorber were employed in a multi-objective optimization procedure aimed at minimizing the heat transfer area requirement and the ammonia/water pressure drop for both components. The optimization was framed by using the MALTAB built-in algorithm *gamultiobj* [10], with an initial population size of 50 elements. The optimization variables were defined as the PHE geometrical specifications that were input to the design model, namely plate corrugation geometry, plate width W and number of channels N_{ch}. The corrugation geometry was defined by the corrugation height b and pitch Λ, and by the chevron angle β. Fig. 3 shows a schematic of the main geometry parameters. The design variables were bounded to lower and upper limits in order to ensure feasible solutions as optimization output. The variables and the bounds are reported in Table 2. Note that the plate length is not reported, since it is the output of the design model: each combination of design variables corresponded to the length needed to meet the design load at absorber and desorber. Two different and separate optimization procedures were carried out for each component.

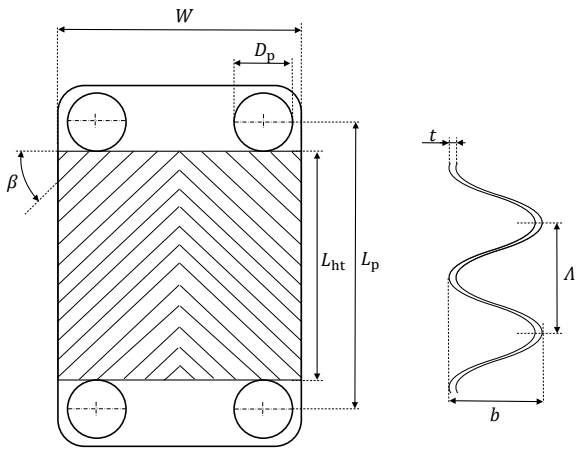

Figure 3: Schematic of PHE geometry

Table 2: Optimization variables and bounds

Variable	Unit	Bounds
W	m	0.040 - 1.100
N_{ch}	-	7 - 200
b	mm	1 - 5
Λ/b	-	1 - 4
β	°	20 - 70

3. Results

This section presents the main results of the study. First, the design of the HACHP considering the set BCs is presented in subsection 3.1.. The output of the geometrical optimization of both absorber and desorber and the impact on COP is introduced in subsection 3.2. Finally, subsection 3.3. reports some suggested optimal designs, discussing similarities and differences.

3.1. HACHP cycle design

Table 3 reports all the thermodynamic state points of the single-stage HACHP, following the numbering of Fig.2, for both the ammonia/water mixture and the heat source and sink. A rich

solution of ammonia/water enters the desorber at the conditions of state point 9 and leaves at state point 1, with vapour quality q (determined by the ammonia vapour in the mixture) increasing from 0.13 up to 0.61. Absorber inlet and outlet are instead given by state points 6 and 5, respectively, with inlet vapour quality of 0.57 and outlet as saturated liquid. Table 4 shows the design heat flow rates in the HEXs, as well as the work required by compression and pumping. Note that these values must be corrected by the electric motor efficiency for the estimation of the COP, reported in the last column of Table 4. The COP, equal to 6.4, was estimated without accounting for pressure drops in any of the components. Note that, given the high ammonia mass fraction considered in the case study, pressures over 20 bar were obtained for both low and high pressure sides. The use of a high pressure compressor, available for ammonia applications up to 50 bar, would thus be required for this system.
The inlet and outlet of absorber and desorber, together with design heat flow rates and mass flow rates, were used as inputs for the PHE sizing in the optimization procedure, and they are noted in Table 3 with bold numbering.

Table 3: HACHP thermodynamic state points

Variable	Thermodynamic state point																
	ammonia/water												sink			source	
	1	2	3	4	**5**	**6**	7	8	**9**	10	11	12	13	14	15	16	17
$\dot{m}$, kg/s	0.13	0.08	0.08	0.08	0.13	0.13	0.13	0.13	0.13	0.05	0.05	0.05	1.00	1.00	1.00	1.72	1.72
T, °C	70	70	141	102	103	92	92	85	60	70	71	89	80	97	100	75	65
p, bar	22.5	22.5	45.7	45.7	45.7	45.7	45.7	45.7	22.5	22.5	45.7	45.7	20.0	20.0	20.0	20.0	20.0
q, -	0.61	1	1	1	0.57	0	0	0	0.13	0	0	0	-	-	-	-	-

Table 4: Output of HACHP cycle design

$\dot{Q}_{\text{abs}}$ kW	$\dot{Q}_{\text{des}}$ kW	$\dot{Q}_{\text{GC}}$ kW	$\dot{W}_{\text{comp}}$ kW	$\dot{W}_{\text{pump}}$ kW	$\dot{Q}_{\text{IHEX}}$ kW	COP -
72.8	72.2	11.3	11.6	0.3	4.8	6.4

3.2. Heat transfer area and pressure drop trade-off

After carrying out the cycle design, the geometry of both PHE absorber and desorber was optimized. Fig. 4 (a) and (b) report the Pareto fronts, e.g. the trade-off between heat transfer area and pressure drop for absorber and desorber, respectively. Each point corresponds to one specific combination of the design variables reported in Table 2. The definition of an optimal trade-off was necessary in order to identify possibilities for optimal design points. This was done by evaluating the impact of ammonia/water pressure drop on the HACHP COP.
Fig. 4 (c) shows the COP degradation due to pressure drop in both the absorber and desorber. The COP is scaled with respect to the design value. First of all, pressure drops in both components imply a linear degradation of the thermodynamic performance. Moreover, the different slopes of the two curves represent the different sensitivity of the heat pump COP to the absorber and desorber design. Absorber pressure drop entails in fact a lower degradation

of the performance, and the optimal design regions of the two Pareto fronts shown in Fig.4 (a) and (b) are defined by different ranges of maximum pressure drop.
Table 5 reports the pressure drops at absorber and desorber related to different percentages of COP degradation. The values were solely related to pressure drop in one component at a time. The maximum allowable pressure drop can therefore be defined for each component by a maximum allowable COP reduction. As an example, if the COP during operation must be kept to a maximum of 1 % deviation with respect to the design value, a design leading to pressure drop lower than 35 kPa and 15 kPa must be chosen for the absorber and desorber, respectively. Note that these values are both consistently lower than maximum pressure drop commonly suggested by manufacturers for many applications.

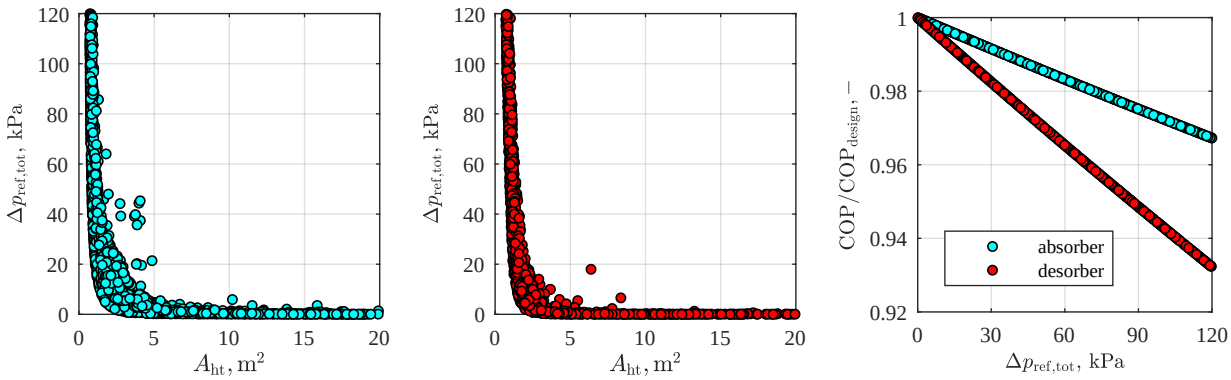

(a) Absorber (b) Desorber (c) Impact on COP

Figure 4: Trade-off heat transfer area and pressure drop for absorber (a) and desorber (b); impact of refrigerant pressuure drop on COP (c)

Table 5: COP degradation implied by different pressure drop at absorber and desorber

COP reduction	Δp_{abs}, kPa	Δp_{des}, kPa
1 %	35	15
2 %	70	35
4 %	145	70
10 %	400	180

3.3. Optimal designs

Table 6 and 7 report some of the optimal design points chosen according to the criteria presented in subsection 3.1., for absorber and desorber, respectively. Six designs were chosen for each component, and listed according to increasing heat transfer area in the tables. Corrugation geometry, plate size and count as well as the resulting trade-off between heat transfer area and pressure drop, are reported. The designs were selected by limiting the pressure drop

below 35 kPa and 15 kPa, in order to ensure a COP degradation lower than 1 % caused by each component. These designs do not constitute all the optimal design points that can be extracted from the Pareto fronts. They represent however different examples of combination of design variables leading to optimal solutions. Moreover, a post-processing screening was carried out, in order to ensure feasible solutions in terms of length-to-width ratio, set to the minimum value of 1.2. The designs with the lowest size respecting the pressure drop limitation were indicated as A-I and D-I for absorber and desorber, respectively, while the other five designs were chosen among the possible solutions with heat transfer area lower than 3 m^2.

Table 6: Optimal absorber designs

Design	Corrugation geometry				Plate size and count				Design trade-off	
	b	Λ	Λ/b	β	W	L_{ht}	L_{ht}/W	$N_{\mathrm{ch,tot}}$	A_{ht}	$\Delta p_{\mathrm{ref,tot}}$
	mm	mm	-	°	m	m	-	-	m^2	kPa
A-I	2.0	2.2	1.1	27	0.093	0.206	2.2	39	1.6	27.1
A-II	3.7	3.8	1.0	20	0.241	0.418	1.7	8	1.9	30.6
A-III	3.5	3.6	1.0	20	0.245	0.310	1.3	14	2.5	14.0
A-IV	4.9	5.0	1.0	20	0.241	0.575	2.4	8	2.6	23.3
A-V	2.4	3.5	1.4	26	0.059	0.241	4.1	113	2.9	9.5
A-VI	4.9	5.1	1.0	20	0.243	0.527	2.2	10	2.9	16.8

Table 7: Optimal desorber designs

Design	Corrugation geometry				Plate size and count				Design trade-off	
	b	Λ	Λ/b	β	W	L_{ht}	L_{ht}/W	$N_{\mathrm{ch,tot}}$	A_{ht}	$\Delta p_{\mathrm{ref,tot}}$
	mm	mm	-	°	m	m	-	-	m^2	kPa
D-I	1.4	1.6	1.1	23	0.132	0.166	1.3	32	1.5	13.7
D-II	2.9	3.5	1.2	26	0.166	0.428	2.6	14	2.0	11.8
D-III	4.3	5.1	1.2	26	0.168	0.715	4.3	11	2.5	11.6
D-IV	1.1	2.3	2.0	27	0.079	0.145	1.8	149	2.5	2.3
D-V	1.5	3.1	2.2	44	0.159	0.293	1.8	42	2.8	5.9
D-VI	3.9	4.8	1.2	26	0.209	0.552	2.6	12	2.8	5.5

By looking at both tables, the optimal corrugation geometry was found to be similar for both components. Even though the pitch-to-height ratio Λ/b was varied between 1 and 4, the optimal configurations resulted in values between 1 and 2, with a maximum of 2.2 for desorber configuration D-V. On the other hand, values of b and Λ ranging from 1 mm up to 5 mm were obtained. The designer must keep in mind that corrugation geometry is often a parameter limited by the commercially available chevron plates. Therefore, depending on the corrugation geometry employed by the chosen manufacturer, different solutions from Table 6 and 7 could be selected. Note that A-I and D-I, corresponding to minimum heat transfer area, were obtained with values of b and Λ around 2 mm and 1.5 mm, respectively. Low b and Λ imply lower hydraulic diameters, thus a better heat transfer performance and higher pressure drop.

The corrugation geometry is also characterized by the chevron angle β. Values of chevron angle close to the lower bound selected for the optimization process, i.e. 20 °, were obtained (with the exception of D-V). Lower chevron angles are usually indicated as *high turbulence* and *high pressure drop* designs. Tables 6 and 7 indicate that it is recommended to choose a low value of chevron angle, since it is possible to tune the remaining design parameters to respect the maximum allowable pressure drop. Moreover, due to the higher pressure drop limitation chosen for the absorber design (35 kPa against 15 kPa), four out of the six designs corresponded to the lower bound of the optimization process (see Table 2). On the other hand, slightly higher values of chevron angle were obtained for the desorber, with D-V reporting a value of 44 °.
The plate size designs obtained for both absorber and desorber were found in different ranges, with length-to-width ratio going from low values of 1.3 up to 4.1-4.3. Tables 6 and 7 therefore suggest that it is possible to choose plate sizes similar to commercially available plates. The number of channels obtained was dependent on the chosen design. Few channels (e.g. A-II, A-IV, D-III and D-VI) entail lower free flow area for the refrigerant, thus higher pressure drop compared to design with similar plate sizes and more plates. The design with a high number of channels (A-V and D-IV) corresponds however to very low pressure drop but higher heat transfer area. The design corresponding to the lowest heat transfer area A-I and D-I were found with a similar number of channels, equal to respectively 39 and 32.

4. Discussion

The results presented in this paper were obtained for a case study of single-stage HACHP for defined temperature lift, ammonia mass fraction and circulation ratio. They are intended to serve as an example of how the optimization of the PHE geometry could be carried out for both absorber and desorber. Moreover, the impact of pressure drop on COP was estimated and used as a criterion to define an optimal trade-off between heat transfer area and pressure drop. Applying the same limits in terms of maximum allowable pressure drop to other types of applications is not trivial. Moreover, different criteria could potentially be used in order to select allowable pressure drop, e.g. by carrying out an economic analysis to study the effect of pressure drop on the levelized cost of heat. This work however stresses the importance of selecting optimized configurations of PHE to install in experimental set-ups, thus a similar methodology is recommended to define the PHE geometry.
Previous experimental campaigns [2, 3] showed that maldistribution issues are one relevant problem hindering the installation of PHE absorber and desorbers as single-units. Previous research on maldistribution in PHEs [22] additionally showed that performance degradation due to maldistribution effects is closely related to the refrigerant sensitivity to pressure drop. As part of future work, it would thus be relevant to evaluate how pressure drop for ammonia/water mixtures affects the sensitivity to liquid/vapour maldistribution.
This study was based on numerical models discretized in 1D, without accounting for fluid flow distribution along the plate width. Therefore, designs with very different length-to-width ratios (e.g. 4.3 of D-III and 1.3 of D-I), were compared by assuming the same ideal refrigerant distribution in both cases. This is not necessarily true in real applications, when designs with low length-to-width ratios could be subject to non-uniform distribution along the plate width. This was considered in the study by posing a limitation on a minimum length-to-width ratio

equal to 1.2. It would however be relevant to understand the minimum length-to-width ratio necessary to ensure proper distribution of the ammonia/water mixture along the entire width.

5. Conclusions

This paper presented a combined HACHP and PHE simulation framework that can be used for (i) cycle design, (ii) PHE absorber and desorber design optimization and (iii) the definition of a optimal trade-off between heat transfer and pressure drop. The application of the framework was illustrated by applying it to a case study of a single-stage HACHP to supply heat at 100 °C with a 25 K temperature lift. The impact of pressure drop on the cycle COP served to establish a criterion of maximum allowable pressure drop for the specific application. 35 kPa and 15 kPa resulted to be the limits for absorber and desorber designs, respectively, leading to a maximum COP degradation of 1 %. All the geometrical specifications of PHE absorber and desorber were optimized and different optimal designs were presented. For the chosen case study, it was found that almost all designs corresponded to the lowest bound set for the chevron angle, while corrugation geometry with different values of pitch and height were obtained. The designs minimizing the heat transfer area resulted however in low b and Λ, thereby enhancing the heat transfer at the expenses of higher pressure drop. Different combinations of plate size in terms of width and length were instead obtained. The presented framework can be applied to other case studies to obtain optimal designs of PHE absorbers and desorbers for HACHPs. The optimized designs serve as a starting point to test single-units PHE absorber and desorber, thus aiming at reducing the installation costs of HEXs in these systems.

Acknowledgments

The research work was funded by Innovations Fund Denmark with the project title THERM-CYC: *Advanced thermodynamic cycles utilizing low temperature heat sources*, and by EUDP (Energy Technology Development and Demonstration) with the project title *Development of ultra-high temperature hybrid heat pump for process application* (grant number: 64011-0351).

Nomenclature

A_{ht}	heat transfer area, m^2
b	corrugation height, mm
COP	coefficient of performance, -
f	circulation ratio, -
L_{ht}	heat transfer length, m
$\dot{m}$	mass flow rate, kg/s
N_{ch}	number of channels, -
n	number of control volumes, -

p	pressure, bar
q	vapour quality, -
$\dot{Q}$	heat flow rate, kW
T	temperature, °C
W	plate width, m
x_r	mass fraction of the rich solution, -

Abbreviations and acronyms

BC	boundary condition
ga	genetic algorithm
GC	gas cooler
HACHP	hybrid absorption compression heat pump
HEX	heat exchanger
IHEX	internal heat exchanger
PHE	plate heat exchanger

Greek symbols

β	chevron angle, °
Δ	difference, -
ϵ	thermal effectiveness, -
Λ	corrugation pitch, mm
η	efficiency, -

Subscripts and superscripts

abs	absorber
des	desorber
el	electric
GC	gas cooler
hs	heat source

in	inlet
is	isentropic
out	outlet
ref	refrigerant

REFERENCES

[1] H. Lorenz. Beiträge zur beurteilung von kühlmaschinen. *Zeitschrift des Vereines Deutscher Ingenieure*, 38(3, 4, 5):62–68, 98–103, 124–130, 1894.

[2] S.R. Nordtvedt. *Experimental and theoretical study of a compression/absorption heat pump with ammonia/water as working fluid.* Phd thesis, Norwegian University of Science and Technology, 2005.

[3] J. Kim, S.R. Park, Y.J. Baik, K. Chang, H.S. Ra, M. Kim, and Y. Kim. Experimental study of operating characteristics of compression/absorption high-temperature hybrid heat pump using waste heat. *Renewable Energy*, 54:13–19, 2013.

[4] J.K. Jensen, W.B. Markussen, L. Reinholdt, and B. Elmegaard. On the development of high temperature ammonia-water hybrid absorption-compression heat pumps. *International Journal of Refrigeration*, 58:79–89, 2015.

[5] J.K. Jensen, T. Ommen, W.B. Markussen, L. Reinholdt, and B. Elmegaard. Technical and economic working domains of industrial heat pumps: Part 2 - Ammonia-water hybrid absorption-compression heat pumps. *International Journal of Refrigeration*, 55:183–200, 2015.

[6] C. Liu, Y. Jiang, W. Han, and Q. Kang. A high-temperature hybrid absorption-compression heat pump for waste heat recovery. *Energy Conversion and Management*, 172(July):391–401, 2018.

[7] M.B. Wersland, T. Eikevik, and I. Tolstorebrov. Investigation of a Hybrid Compression Absorption Heat Pump System for High Temperatures. In *Proceedings of 13th IIR Gustav Lorentzen Conference on Natural Refrigerants, Valencia*, 2018.

[8] Hybrid Energy AS. High temperature heat pumps. `https://www.hybridenergy.no/reference-plants/`. [accessed: 11.02.2019].

[9] J.K. Jensen. *Industrial heat pumps for high temperature process applications.: A numerical study of the ammonia-water hybrid absorption-compression heat pump.* Phd thesis - dcamm special report no.s207, Technical Unviersity of Denmark, 2016.

[10] Mathworks. gamultiobj, Matlab 2017b. `https://www.mathworks.com/help/gads/gamultiobj.htm`. [accessed: 11.02.2019].

[11] R. Mancini, B. Zühlsdorf, J.K. Jensen, W.B. Markussen, and B. Elmegaard. Deriving guidelines for the design of plate evaporators in heat pumps using zeotropic mixtures. *Energy*, 156, 2018.

[12] E.W. Lemmon, I.H. Bell, M.L. Huber, and M.O. McLinden. NIST Standard Reference Database 23: Reference Fluid Thermodynamic and Transport Properties - REFPROP, version 10.0. 2018.

[13] H. Martin. A theoretical approach to predict the performance of chevron-type plate heat exchangers. *Chemical Engineering and Processing: Process Intensification*, 35(4):301–310, 1996.

[14] F. Táboas, M. Vallès, M. Bourouis, and A. Coronas. Assessment of boiling heat transfer and pressure drop correlations of ammonia/water mixture in a plate heat exchanger. *International Journal of Refrigeration*, 35(3):633–644, 2012.

[15] L. Silver. Gas cooling with aqueous condensation. *Industrial Chemist and Chemical Manufacturer*, 23(269):380–386, 1947.

[16] K.J. Bell and M.A. Ghaly. An approximate generalized design method for multicomponent/partial condenser. *AIChE Symposium Series*, 69:72–79, 1973.

[17] J. Zhang, M. R. Kærn, T. Ommen, B. Elmegaard, and F. Haglind. Condensation heat transfer and pressure drop characteristics of R134a, R1234ze(E), R245fa and R1233zd(E) in a plate heat exchanger. *International Journal of Heat and Mass Transfer*, 128:136–149, 2019.

[18] R.W. Lockhart and R.C. Martinelli. Proposed correlation of data for isothermal two-phase, two-component flow in pipes. *Chemical engineering progress*, 45(1):39–48, 1949.

[19] M. Conde-Petit. Thermophysical properties of NH3+H2O Mixtures for Industrial Design of Absorption Refrigeration Equipment. `http://www.mrc-eng.com/`, 2006. [accessed: 13.02.2019].

[20] C.R. Wilke. A viscosity equation for gas mixtures. *The Journal of Chemical Physics*, 18(4):517–519, 1950.

[21] E.A. Mason and S.C. Saxena. Approximate formula for the thermal conductivity of gas mixtures. *Physics of Fluids*, 1(5):361–369, 1958.

[22] R. Mancini, B. Zühlsdorf, V. Aute, W.B. Markussen, and B. Elmegaard. Performance of heat pumps with pure and mixed refrigerants with maldistribution effects in plate heat exchanger evaporators. *submitted to International Journal of Refrigeration*, 2019.